

Quantum capacitive phase detector

Leif Roschier,* Mika Sillanpää, and Pertti Hakonen

Low Temperature Laboratory, Helsinki University of Technology, P. O. Box 2200, FIN-02015 HUT, Finland

(Received 22 July 2004; revised manuscript received 1 October 2004; published 31 January 2005)

We discuss how a single Cooper-pair transistor may be used to detect the superconducting phase difference by using the phase dependence of the input capacitance from gate to ground. The proposed device has a low power dissipation because its operation is in principle free from quasiparticle generation. According to the sensitivity estimates, the device may be used for efficient qubit readout in a galvanically isolated and symmetrized circuit.

DOI: 10.1103/PhysRevB.71.024530

PACS number(s): 85.35.Gv, 73.23.Hk, 85.25.Cp

The interest in Coulomb blockade and accompanying quantum effects due to superconductivity has triggered a wave of research on the physics and future applications. One basic device¹ is the single-electron transistor (SET) which consists of two small tunnel junctions having a sum capacitance of C_Σ . If the single-electron charging energy $E_C = e^2/(2C_\Sigma)$ dominates over temperature, $E_C \gg k_B T$, the SET works as the most sensitive known electrometer.

In order to gain advantage of the inherently large bandwidth $(R_{\text{SET}}C_\Sigma)^{-1} \sim 10$ GHz of the SET charge detector, two technologies have been developed where the SET is read using an LC oscillator. The rf-SET (radio-frequency SET) is based on the gate dependence of the differential resistance of a sequential tunneling SET, a property that modulates the Q value of the oscillator.² No other device than the rf-SET has been able to track dynamic single-charge transport at megahertz frequencies, which is relevant especially from the point of view of characterization and eventual single-shot readout of superconducting qubits.³

Because of the limitations due to the dissipative nature of the rf-SET, a technique called L-SET (inductive SET), having low dissipation, has been developed recently.⁴ With zero dc-voltage, a superconducting SET, henceforth called a single-Cooper-pair transistor (SCPT), behaves as an energy-storing reactive component because of the Josephson coupling ($E_J/2$ is defined as the single-junction Josephson energy).

Since the first energy band E_0 of the SCPT grows approximately quadratically as a function of the drain-source phase difference ϕ , the SCPT behaves as an inductor when looked at from the source or drain. The effective Josephson inductance of a SCPT, $L_J^{-1} = (2\pi/\Phi_0)^2 \partial^2 E_0 / \partial \phi^2$, has a strong dependence on the (reduced) gate charge $n_g = C_g V_g / (2e)$ if $E_J/E_C \ll 1$. Here, $\Phi_0 = h/(2e)$ is the flux quantum. In the L-SET schematics, a charge detector is built so that the resonance frequency of a system of a SCPT and an LC tank depends on n_g . So far, we consider the L-SET the most promising method of sensitive and fast electrometry.

In addition to resistance or inductance, capacitance remains in the group of linear circuit elements. The first energy band of a SCPT grows approximately quadratically also with respect to the second external parameter n_g . (A corresponding statement holds also for a single junction, which has been suggested in Ref. 5 as a capacitance tunable by injected

charge.) Therefore, while observed from the gate electrode, the SCPT looks like an effective capacitance C_{eff} to ground. The operational principle of our proposal is based on the dependence of C_{eff} on the source-drain phase difference ϕ ,

$$C_{\text{eff}}(\phi)^{-1} \equiv \frac{\partial V_g}{\partial q_g(\phi)}, \quad (1)$$

where q_g is the charge on the gate capacitor, as illustrated in Figs. 1(a) and 1(b). Note that in general $q_g \neq C_g V_g$.

Once coupled to a tank circuit, modulation of $C_{\text{eff}}(\phi)$ can be used to read a phase difference (henceforth, called simply a phase) reactively in a reflection measurement (see Fig. 1). The phase is defined as the time integral of the voltage, $\phi = (2\pi/\Phi_0) \int_0^t V dt'$. In the superconducting case, ϕ equals the order parameter phase.

Unlike any previous considerations of single-electron or single-Cooper-pair devices, the ‘‘quantum capacitive phase detector’’ device proposed in the present paper is a generally fast and sensitive *phase* detector. We call the device a CSET, to emphasize its somewhat dual operation with respect to the L-SET device.

The Hamiltonian for a SCPT symmetric in its Josephson energies is⁶

$$H = E_{\text{CP}} \left(\frac{\partial}{i \partial \theta} - n_g \right)^2 - E_J \cos(\phi/2) \cos(\theta), \quad (2)$$

where a term $C_g V_g^2/2$ and terms having ϕ have been ignored. $E_{\text{CP}} \equiv (2e)^2/(2C_\Sigma)$ is the Cooper-pair charging energy and

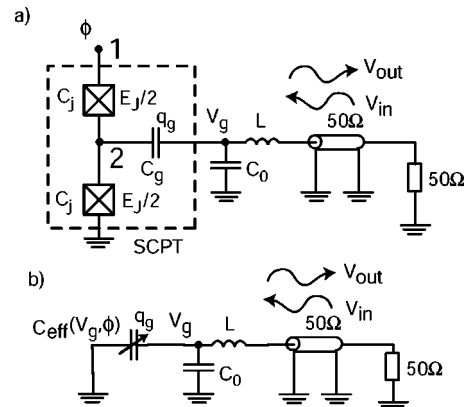


FIG. 1. (a) CSET circuit. (b) An equivalent circuit.

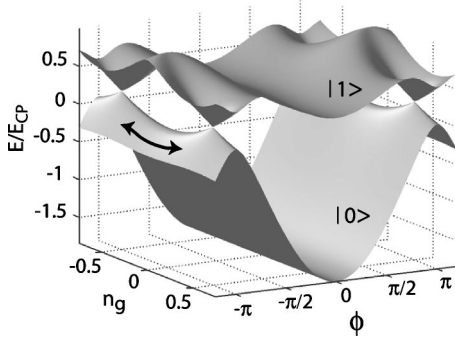


FIG. 2. The lowest ($|0\rangle$) and the first excited ($|1\rangle$) energy surfaces for a symmetric SCPT ($d=0$) with $E_J/E_{CP}=3$. The black line denotes the CSET operation point $\phi \sim \pi$ and $V_g(t) = V_{g0} \cos \omega_0 t$.

$E_J/2$ is the Josephson coupling energy of the individual junctions. The phases are defined with the help of voltages V_i at points 1 and 2 in Fig. 1: $\theta = (2\pi/\Phi_0) \int_0^t (V_1/2 - V_2) dt'$ and $\phi = (2\pi/\Phi_0) \int_0^t V_1 dt'$. Here, the former is the difference and the latter is the sum of the phases over the two Josephson junctions.

The eigenvalues for this Hamiltonian are given by the solutions to the Mathieu equation when $n_g \neq n/2$, where n is integer.^{6,7}

$$E_k(\phi, n_g) = \frac{E_{CP}}{4} \mathcal{M}_{\mathcal{A}} \left(k+1 - (k+1)[\text{mod } 2] + 2n_g(-1)^k, \frac{2E_J \cos(\phi/2)}{E_{CP}} \right), \quad (3)$$

where $\mathcal{M}_{\mathcal{A}}(r, q)$ is the characteristic value \mathcal{A} for even Mathieu functions⁸ with characteristic exponent r and parameter q . The unavoidable asymmetry of tunnel junctions in a real device is easily incorporated into Eq. (3). By substituting $\frac{E_J \cos(\phi/2)}{E_J \sqrt{[1+d^2 + (1-d^2) \cos(\phi)]/2}}$ in Eq. (3) by $E_J \sqrt{[1+d^2 + (1-d^2) \cos(\phi)]/2}$, we get energies of a SCPT whose individual junctions have unequal Josephson energies $E_J(1+d)/2$ and $E_J(1-d)/2$, where $d \neq 0$ is the asymmetry parameter. Junction capacitances, however, can be arbitrarily distributed. Figure 2 illustrates the two lowest eigenvalues E_0 and E_1 with respect to the control parameters ϕ and n_g .

In order to calculate the observable capacitance C_{eff} from gate to ground when the system is in the lowest eigenstate E_0 , we calculate $q_g = C_g(V_g - V_2)$, where the island voltage is $V_2 = 1/C_g(\partial E_0/\partial V_g)$. Using Eq. (1) we have

$$C_{\text{eff}} = \frac{\partial}{\partial V_g} \left(C_g V_g - \frac{\partial E_0}{\partial V_g} \right) = C_g - \frac{C_g^2}{C_Q}, \quad (4)$$

where C_Q is the quantum capacitance $C_Q^{-1} \equiv (\partial^2 E_0)/[(2e)^2 \partial n_g^2]$ due to the SCPT band structure. In the following analysis, the constant term C_g is neglected, because it is small compared with the shunting capacitance C_0 .

In order to get maximum performance of the phase detector, we take the operation point of the device such that the transfer function $\partial C_{\text{eff}}/\partial \phi$, which is the derivative of the capacitance modulation curves in Fig. 3, is maximized. This happens at ϕ rather close to π . As seen in Fig. 3, the transfer

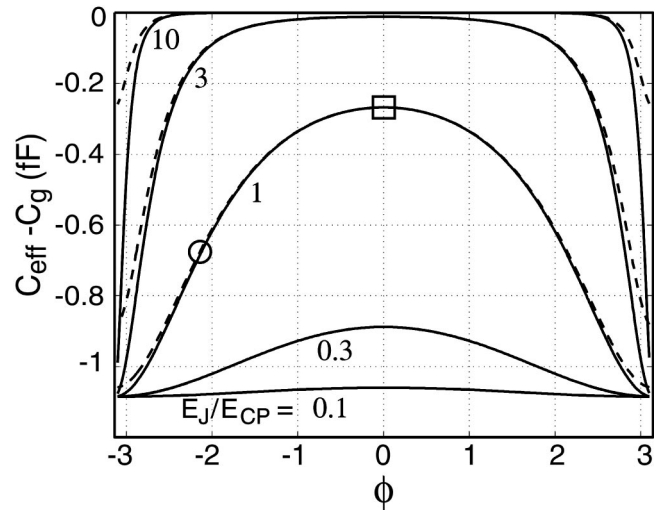


FIG. 3. Capacitances C_{eff} calculated using Eq. (4) with $C_g = 2$ fF and $E_{CP} = 1$ K. Solid lines are for a symmetric SCPT ($d=0$), and the dashed lines for a slightly asymmetric SCPT ($d=0.1$). The numbers denote the E_J/E_{CP} ratio. The circle and the square correspond to the operation points marked in Fig. 6 below for the charge-phase qubit readout.

function increases rapidly at large E_J/E_{CP} . The price to pay for a high gain then is a limited dynamic range. The external gate drive is taken as $V_g(t) = V_{g0} \cos \omega_0 t$.

Asymmetry in the SCPT weakens the modulation considerably at high $E_J/E_{CP} \gtrsim 3$ as seen in Fig. 3 (dashed lines). This is because asymmetry removes the degeneracy at $n_g = \pm 0.5$ and $\phi = \pm \pi$ and smooths out the strongest modulation.

As seen in Fig. 1(b), the proposed CSET circuit is a series resonator with inductance L and total capacitance $C = C_0 + C_{\text{eff}}$. The resonance frequency f of the configuration is then tunable by C_{eff} . A shift of f due to a change of capacitance ΔC is

$$f = f_0 + \Delta f \propto \frac{1}{\sqrt{C_0 + \Delta C}} \approx \frac{1}{\sqrt{C_0}} - \frac{\Delta C}{2C_0^{3/2}}, \quad (5)$$

and we find $\Delta f/f_0 \approx -\Delta C/2C_0$. ΔC can be written in terms of a phase change $\Delta \phi$ as $\Delta C = (\partial C_{\text{eff}}/\partial \phi) \Delta \phi$. For simplicity, we choose $\Delta \phi = 1$ rad.

We assume that the resonator itself does not dissipate power so that its internal quality factor $Q_i = \infty$. The loaded Q factor $Q^{-1} = 1/Q_i + 1/Q_e$ is then set by the external impedance $Z_0 = 50 \Omega$, so that $Q = Q_e = \omega L/Z_0 = \sqrt{L/C}/Z_0$. This is a good approximation with low Q . It follows that the phase $\vartheta = \arg(V_{\text{out}}/V_{\text{in}})$ of the voltage wave amplitude reflected from the resonator, as illustrated in Fig. 1, changes by π in the frequency range of $\sim f_0/Q$. At the resonant frequency, the differential change of phase is larger, and by direct calculation one gets the maximum modulation $\Delta \vartheta/\Delta f = 4Q/f_0$, and

$$\Delta \vartheta \approx -\frac{2Q\Delta C}{C_0} = -\frac{2\Delta C\sqrt{L}}{C_0^{3/2}Z_0}. \quad (6)$$

We assume operation safely in the linear regime, such that the gate charge amplitude is at maximum of the order $e/2$,

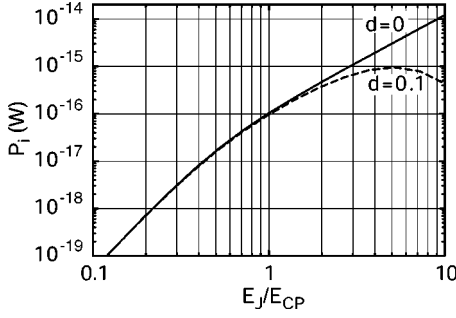


FIG. 4. Information power [Eq. (10)] corresponding to a phase modulation $\Delta\phi=1$ rad. Solid line, symmetric SCPT ($d=0$); dashed line, slightly asymmetric SCPT ($d=0.1$). Other parameters are as given in the text.

and thus the gate voltage amplitude is $V_{g0} \approx e/2C_g$. The average energy stored in the capacitors C_{eff} and C_0 is of the order $E \approx V_{g0}^2(C_{\text{eff}} + C_0)/2 = e^2 C / (8C_g^2)$. Because it takes Q cycles for the (loaded) resonator to dissipate most of its stored energy, the reflected power flow is

$$P \approx Ef_0/Q = \frac{f_0 e^2 C}{8QC_g^2}. \quad (7)$$

This is about 5 fW with typical parameters in an experiment. The voltage amplitude of the modulation is $\Delta V = \Delta \partial V_c$, where the carrier voltage amplitude is $V_c = \sqrt{2Z_0 P}$. The modulation is conveniently transformed into power units to enable later comparison with noise power. This leads to the definition of information power:

$$P_i \equiv \frac{(\Delta V)^2}{2Z_0} = \frac{(\Delta \partial)^2 V_c^2}{2Z_0} = (\Delta \partial)^2 P. \quad (8)$$

By combining Eqs. (6), (7), and (8), we find

$$P_i \approx Q \left(\frac{\Delta C}{C_0} \right)^2 \frac{f_0 e^2 C}{2C_g^2}. \quad (9)$$

Equation (9) may be written in terms of the transfer function $\partial C_{\text{eff}}/\partial\phi = C_g^2 \partial^3 E_0 / (4e^2 \partial n_g^2 \partial\phi)$, C_0 , and Z_0 . We also approximate $C_{\text{eff}} \ll C_0$. It follows that

$$P_i(\Delta\phi) \approx \frac{1}{64\pi Z_0 e^2} \left(\frac{\partial^3 E_0}{\partial n_g^2 \partial\phi} \Delta\phi \right)^2 \left(\frac{C_g}{C_0} \right)^2. \quad (10)$$

Sensitivity increases dramatically by increasing the E_J/E_{CP} ratio as is illustrated in Fig. 4. $E_{\text{CP}} \gg k_B T$ must be satisfied in order to keep the system localized in the lowest state E_0 . At a fixed ratio of E_J/E_{CP} , maximization of C_g/C_0 and minimization of Z_0 yields the best sensitivity.

In order to estimate device performance we take the operation frequency f_0 to be ~ 1 GHz. The individual component values are chosen to be easily realizable by present fabrication technology. Due to stray capacitance from bonding pads, etc., it is difficult to achieve in practice C_0 lower than ~ 0.15 pF. To have a series resonance at the f_0 with Q factor of ~ 20 , this would be accompanied by an inductance $L \sim 160$ nH. The inductance may be easily realized by using a commercial surface mount coil. It is to be noted that the

TABLE I. Linearized relative change of capacitance corresponding to a $\Delta\phi=1$ rad, for symmetric SCPT (parameters as in the text).

E_J/E_{CP}	0.1	0.3	1	3	10
$\Delta C/C_0$	8.5×10^{-5}	6.6×10^{-4}	3.6×10^{-3}	1.1×10^{-2}	4.3×10^{-2}

capacitance C_{eff} is $\sim 1/75$ of the capacitance C_0 assuming a large $C_g \sim 2$ fF. The large gate capacitance is easily implemented with a similar overlap junction as the two SCPT tunnel junctions, but using a much longer oxidation to create a highly resistive junction.⁹

For phase sensitivity estimates, we calculated $\Delta C/C_0$ resulting from a phase change $\Delta\phi=1$ rad, at different ratios of E_J/E_{CP} , and assuming $E_{\text{CP}}=1$ K. They are listed in Table I. The values are calculated at the optimal operation point of ϕ which maximizes the transfer function, and at $V_g \sim 0$. As seen in Fig. 4, the information power is $P_i \sim 10$ fW with $E_J/E_{\text{CP}} \sim 10$.

By using a cryogenic HEMT (high electron mobility transistor) amplifier with a typical noise temperature of 3 K that corresponds to spectral density of $s_N \sim 4 \times 10^{-23}$ W/Hz, we find the phase sensitivity $s_\phi = \sqrt{s_N/P_i}$ (1 rad) of the order of $45 \mu\text{rad}/\sqrt{\text{Hz}}$ for symmetric SCPT. Combined with a low-noise superconducting quantum interference device (SQUID) amplifier¹⁰ that would be close to the resonator circuit, the value Z_0 could be lowered to a value of 1Ω or below¹¹ and the noise temperature could be down by a factor of 30. This would result in a sensitivity of $1.3 \mu\text{rad}/\sqrt{\text{Hz}}$.

Asymmetry in the SCPT junctions weakens the numbers at high E_J/E_{CP} , as portrayed by the dashed line in Fig. 4. With $E_J/E_{\text{CP}}=10$ and $d=0.1$, the mentioned sensitivities would go down by a factor of 5. However, at high E_J/E_{CP} the junctions are naturally of large area, and hence relatively easy to fabricate with similar sizes.

For the estimates discussed here, we have assumed operation of the device only at “safe” values of V_g . That is, variation of the capacitance C_{eff} is continuous over a reasonable range of values around the operation point. As evident in Fig. 2, close to the degeneracy points, the differential change of capacitance is substantially larger. One needs, however, a relatively strong ac gate drive V_{g0} in order to distinguish the carrier signal from the pre-amplifier noise power within the bandwidth. For this reason, we have omitted the analysis of these points.

In order to demonstrate an important application of the CSET, we discuss a circuit where the CSET works as a detector for the state of the charge-phase qubit (see Fig. 5).

The basic idea of this circuit is that since the qubit states $|0\rangle$ and $|1\rangle$ correspond to distinct phases ϕ , they result in a different capacitance of the CSET phase detector.

Due to a supposed large capacitance, $C_s \gtrsim 20$ fF, the phases with respect to ground at points A and B are taken as classical variables. The charging energy of these leads is neglected for the same reason. The structure having this high capacitance is naturally fabricated on a ground plane substrate. For a standard insulator thickness of 300 nm on top of a conducting ground plane, the loop structure would measure only tens of micrometers in size.

We assume that the circuit can be described as two connected SCPTs (detector and qubit) and that the gauge-

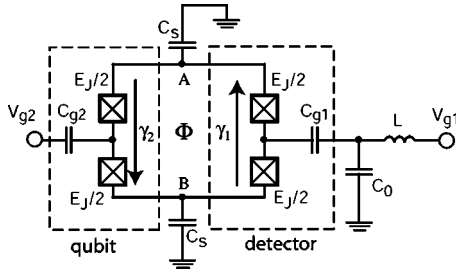


FIG. 5. Schematic of the CSET coupled to a charge-phase qubit (Ref. 12). The gauge-invariant phase differences γ_i and their orientations are marked with arrows. All Josephson junctions are taken to have the same Josephson coupling energy $E_J/2$. Φ is the externally applied magnetic flux.

invariant phase γ_i over each of them is found by solving the equations

$$\gamma_1 + \gamma_2 = -2\pi\Phi/\Phi_0 \pmod{2\pi} \quad (11)$$

and

$$\frac{\partial E_{k'1}(\gamma_1, V_{g1})}{\partial \gamma_1} = \frac{\partial E_{k2}(\gamma_2, V_{g2})}{\partial \gamma_2}. \quad (12)$$

The former equation assures the correct 2π periodicity of the sum of the phases around the loop. The latter equation states that the currents flowing through both SCPTs have the same magnitude. The energies E are defined according to Eq. (3). The band index k' for the detector is always null and the qubit index k takes values 0 or 1, corresponding to the states $|0\rangle$ and $|1\rangle$. For this example we assume for simplicity that both SCPTs have $E_J/E_{CP}=1$.

As an example of the operation we suppose that after manipulating the qubit, it is in a superposition which then collapses into either $|0\rangle$ or $|1\rangle$ when the detector is turned on. The detector, on the other hand, stays in the state $|0\rangle$. In order to start the measurement, the qubit gate voltage is turned to approximately $C_g V_{g2}/2e=0.37$. The detector is maintained at $C_g V_{g1}/2e=0$ throughout the operations. Thereafter, an externally applied magnetic flux is ramped adiabatically to $\Phi/\Phi_0 \approx 1/2$.

Figure 6 illustrates the dependence of γ_1 with respect to the qubit state. Depending on the state of the qubit, the phase over the detector circuit γ_1 will thus become either 0 or ~ -2 rad. According to Fig. 3, the capacitance C_{eff} then differs by ~ 0.4 fF, depending on the qubit final state. According to Eq. (9), the difference corresponds to an information power of -132 dBm, by using easily achievable values $C_0=0.15$ pF, $Q=20$, $f_0=1$ GHz, and $C_g=2$ fF. A signal-to-noise ratio 1 is then achieved at a bandwidth of 20 MHz with a feasible SQUID first-stage amplifier having a noise temperature of 0.3 K. Measurement is thus clearly possible in the submicrosecond regime. A reasonable junction asymmetry $d=0.1$ has a negligible influence on the curves in Fig. 6.

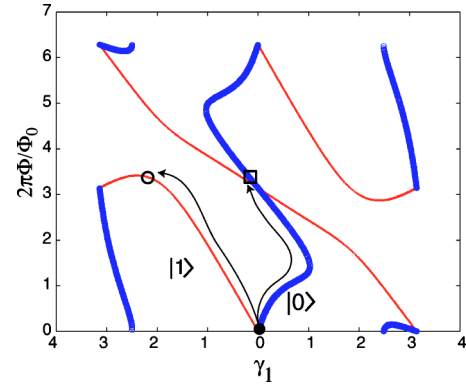


FIG. 6. Dependence of the phase over the detector γ_1 on the applied magnetic flux Φ . The thick lines correspond to the solutions of Eqs. (11) and (12), when the qubit is in the state $|0\rangle$. The thin lines are for the qubit state $|1\rangle$.

The proposed qubit circuitry has several important advantages. First, low power dissipation means low rate of quasi-particle generation, which is essential for low back action and fast recovery from the measurement. Second, since the circuit is galvanically isolated, it is free from external quasi-particle injection.

The third advantage is the symmetry of the schematics. Although in some sense the circuit is strongly coupled to the external Z_0 via the detector gate, the thermal noise of Z_0 acts only as a common-mode signal. This is equivalent to saying that the real part of the impedance seen by the qubit $\text{Re}(Z)$ is very small. Asymmetry weakens the situation, but with a realistic, random asymmetry of about 20% in the component values, we calculated the following figures in the schematics of Fig. 5: $\text{Re}(Z) \ll 1$ m Ω both at low frequency ($f < 1$ GHz) which is relevant for dephasing, and at the level-spacing frequency (10–50 GHz) which affects relaxation. Especially since the qubit operations are naturally performed at the saddle point $\phi=0, n_g = \pm 1/2$, as in the original charge-phase qubit, the system is extremely well decoupled from the environment. Note that the gate and flux operation leads of the qubit may be weakly coupled so that they do not contribute noise.

The coherence time is then presumably limited by internal $1/f$ noise, which should be similar to existing qubit realizations. Its effect weakens as E_{CP} grows. At a conservative value $E_{CP}=1$ K, we estimate a dephasing time¹³ of 1–2 μ s, which is comparable to the original charge-phase qubit.

In conclusion, we have proposed a technique to measure the superconducting phase difference by monitoring the effective capacitance between the gate of a single-Cooper-pair transistor and ground. As a practical example, the readout of a charge-phase qubit using the technique was discussed.

Fruitful discussions with T. Heikkilä, N. Kopnin, and T. Lehtinen are gratefully acknowledged. This work was supported by the Academy of Finland and by the Large Scale Installation Program ULTI-3 of the European Union.

*Electronic address: Leif.Roschier@iki.fi

¹D. Averin and K. Likharev, *J. Low Temp. Phys.* **62**, 345 (1986).

²R. Schoelkopf, P. Wahlgren, A. Kozhevnikov, P. Delsing, and D. Prober, *Science* **280**, 1238 (1998).

³A. Aassime, G. Johansson, G. Wendin, R. Schoelkopf, and P. Delsing, *Phys. Rev. Lett.* **86**, 3376 (2001).

⁴M. Sillanpää, L. Roschier, and P. Hakonen, *Phys. Rev. Lett.* **93**, 066805 (2004).

⁵D. V. Averin and C. Bruder, *Phys. Rev. Lett.* **91**, 057003 (2003).

⁶K. Likharev and A. Zorin, *J. Low Temp. Phys.* **59**, 347 (1985).

⁷A. Cottet, Ph.D. thesis, CEA-Saclay, 2003.

⁸Function *MathieuCharacteristic A*[r, q] in MATHEMATICA.

⁹G. Zimmerli, R. Kautz, and J. Martinis, *Appl. Phys. Lett.* **61**,

2616 (1992).

¹⁰M.-O. André, M. Mück, J. Clarke, J. Gail, and C. Heiden, *Appl. Phys. Lett.* **75**, 698 (1999).

¹¹Input impedance of the microstrip SQUID amplifier is determined by the shunt resistors transformed into amplifier input. Also, a nonstandard way of coupling the input signal is required in the application.

¹²D. Vion, A. Aassime, A. Cottet, P. Joyez, H. Pothier, C. Urbina, D. Esteve, and M. Devoret, *Science* **296**, 886 (2002).

¹³A. Cottet, A. Steinbach, P. Joyez, D. Vion, H. Pothier, D. Esteve, and M. Huber, in *Macroscopic Quantum Coherence and Quantum Computing*, edited by D. V. Averin, B. Ruggiero, and P. Silvestrini (Kluwer/Plenum, Dordrecht, 2001).